



**Research Article**

**ASSESSMENT OF WIND PRESSURE BY EUROCODE-1, TS 498 AND CFD ANALYSES FOR DOUBLE-SLOPED ROOF BUILDING**

**Halil ZEYREK\*<sup>1</sup>, Serkan BEKİROĞLU<sup>2</sup>**

<sup>1</sup>*Yıldız Teknik University, Department of Civil Engineering, ISTANBUL; ORCID: 0000-0003-4723-9863*

<sup>2</sup>*Yıldız Teknik University, Department of Civil Engineering, ISTANBUL; ORCID: 0000-0003-3554-9442*

**Received: 14.08.2018 Revised: 18.12.2018 Accepted: 04.02.2019**

**ABSTRACT**

In this study, building external wall pressures induced by wind velocity for rectangular planned-buildings with several roof slopes are determined using two wind standards such as Eurocode-1 and TS 498 and two-dimensional computational fluid dynamics (CFD) analysis. In CFD analyses, wind velocity function produced according to Eurocode-1 is used as velocity input. At the end of the study, wall pressures obtained by using Eurocode-1, TS 498 and CFD analyses are compared on the same peripheral region of the buildings. It is concluded that the results of TS 498 are not at a sufficient level according to the results of Eurocode-1 and CFD analyses. The results of Eurocode-1 and CFD analyses match with each other regarding positive and negative pressures on the same peripheral region. Eurocode-1 propounds higher values than those of CFD except values obtained on regions at the folded-corners of some buildings.

**Keywords:** Computational fluid dynamics (CFD) analyses, Eurocode-1 (TS EN 1991-1-4), TS 498, rectangular planned to build with double-sloped roof, external wall pressure, wind velocity function.

**1. INTRODUCTION**

Nowadays there is an increase in the number of buildings having different geometries and heights so that the wind-building interaction has become much more important. Determination of the interaction is conducted by invoking experimental and numerical methods. Experimental studies are being undertaken by subjecting many buildings to wind tunnel tests. In this way, the wind load induced effects are determined. Wind tunnel test is preferred especially in extensive projects such as high buildings, bridges, and stadiums. Moreover, the wind loads on buildings are also found using CFD as well as experimental works. The behavior of fluid in motion is determined with CFD using mathematical approaches. There is a lot of computer software available for CFD solutions. By the way, there are many standards for calculating the wind-induced effects in buildings. The standards used in Turkey are the Eurocode-1 (TS EN 1991-1-4) [1], TS 498 (this standard is in force, but TS EN 1991-1-4 is referred for wind calculation) [2] and "İstanbul Yüksek Binalar Rüzgar Yönetmeliği" [3].

Many experimental and numerical studies are available in the literature. For example, Kurç et al. [4] determined the effects of wind on high buildings by wind tunnel tests in their studies. As a result of their studies, they found that the wind effect changes according to the aspect ratio of the

\* Corresponding Author: e-mail: zeyrekhali1@gmail.com, tel: (212) 383 51 90

building, where the impact of wind on the building is reduced as the ratio increases between the dimension of the building in the same direction as the wind to the width of the surface that the wind stroke in a building that has a rectangular cross-section. Özmen and Kaydok [5] have numerically studied the wind effects on high buildings on various cross-sections. In the conclusion of the study, they have determined that the surface pressure distributions in the flow fields of the geometric changes created in the models of high buildings led to significant differences. Furthermore, when they evaluated the sensitivities of turbulence models against experimental results, they observed that the RNG k- $\epsilon$  turbulence model calculated more consistent results with the experimental data. For greenhouses with sloping roofs in different flow types, Vasilios et al. [6] compared the external pressure coefficients numerically by calculating with Eurocode-1. As a result of the study, they found that the analytical pressure coefficients in the negative pressures that form reverse flow regions were higher than the Eurocode-1 pressure coefficients. Ozmen [7] experimentally and theoretically studied the wind effects on buildings with different roof types and slopes. As a result of the study; it was found that there was a positive pressure area in the front walls of all of the buildings, negative pressure on the front surface of the roof, in the buildings with 15° and 30° degrees roof pitch; positive pressure on the front surface of the roof, in the building with a 45° degree roof pitch and negative pressure, was found on the rear roof surface of all of the buildings and the rear front of the buildings. Xing et al. [8] conducted experimental and numerical studies of pressure distributions in buildings that have a cradle roof with and without embrasure. As a result of the study, they observed that the results obtained from experimental and numerical analysis are in conformity with each other and emphasized the importance of the determining the wind effects on the building by the numerical method or wind tunnel test.

At the end of the literature review above, it is seen that despite there are numerous studies in the literature in which the buildings with sloped roofs are examined, there are just a few studies have been found concerning constructions with different roof pitch angles so that the results of numerical analysis and obtained from the standards such as Eurocode-1 and TS 498 can be compared in detail. In this study, four different building examples (see Figure 1) which are rectangular planned and having a duo-pitched roofs with angles of 15°,30°,45° and 60° will be compared using the Eurocode-1 and TS 498 with the results of external wall pressure determined by CFD analyses carried on Ansys Fluent software.

This study includes five sections except for the introduction and conclusion. In section 2, basic information will be given about CFD, Navier-Stokes Theory and turbulence models. In section 3, the results of the external wall pressure will be found for each building according to the five different terrain categories defined in Eurocode-1. In section 4, the results of the external wall pressure will be given according to TS 498. In section 5, CFD analyses will be performed using the Ansys Fluent program. Here, wind velocity functions will be used as input of the analyses for five different terrain categories based on the formulas in Eurocode-1. In section 6, results obtained from Eurocode-1, TS 498 and CFD analyses will be discussed.

## 2. COMPUTATIONAL FLUID DYNAMICS

The branch of science that studies fluid movements is called fluids dynamics. The fluid concept includes both liquids and gases. The fluid dynamics are examined in three main branches such as the experimental fluid dynamics, theoretical fluid dynamics, and computational fluid dynamics (CFD).

There are many CFD software based on a method such as Finite Volume Method (FVM), Finite Difference Method (FDM) and Finite Element Method (FEM) which are utilized to determine the physical behavior of the fluid and to convert analytical solution to a numerical solution. The CFD software is preferred to do away with the need for experimentation since experimental studies require high cost and long time.

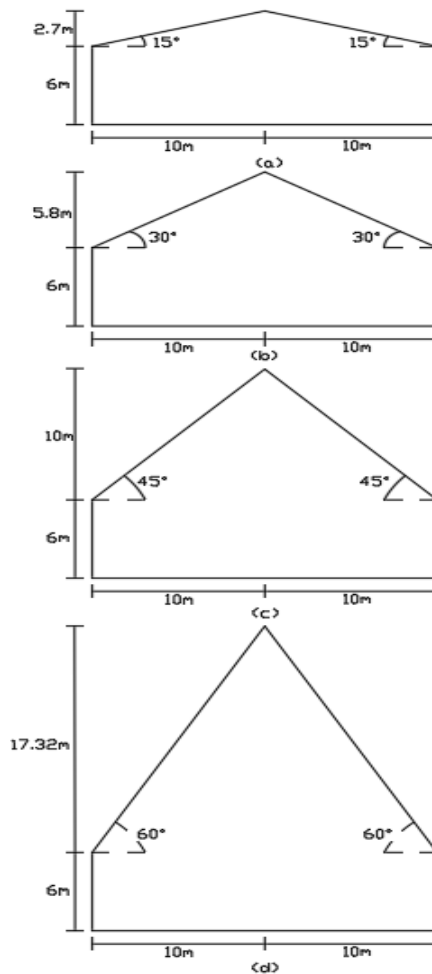


**Figure 1.** Examples of building s within 15°, 30°, 45° and 60° degrees duo-pitched roofs

The current state of computational fluid dynamics is that CFD can cope a laminar flow with ease, but turbulent flows of practical engineering interest are impossible to solve without invoking turbulence models. However, there is no universal turbulence model, and a turbulent in CFD solution is just as good as the suitability of the turbulence model. Even so limitation, the standard turbulence models yield reasonable results for a lot of practical engineering problems [9].

### 2.1. The Navier-Stokes Theory

Fluid motion is solved using basic conservation equations such as mass, momentum, and energy conservation equations. The Navier-Stokes equations are derived from these equations. Physical behavior of fluid motion is determined as a result of solving the derived equations. The Navier-Stokes equations involve complex and nonlinear expressions. Because of this, the analytical solution is quite difficult. The solution of Navier-Stokes equations is realized numerically in computer software.

Three-dimensional continuity, momentum, and energy differential equations that form Navier-Stokes Equations 1-2-3 are shown below, respectively.

Continuity equation:

$$\frac{\partial p}{\partial t} + \frac{\partial(pu)}{\partial x} + \frac{\partial(pv)}{\partial y} + \frac{\partial(pw)}{\partial z} = 0 \quad (1)$$

Momentum equation for the direction of x:

$$\frac{\partial(pu)}{\partial t} + \frac{\partial(puu)}{\partial x} + \frac{\partial(pvu)}{\partial y} + \frac{\partial(pwu)}{\partial z} = \frac{\partial\sigma_{xx}}{\partial x} + \frac{\partial\tau_{yx}}{\partial y} + \frac{\partial\tau_{zx}}{\partial z} \quad (2)$$

Energy equation:

$$\frac{\partial(pE)}{\partial t} + \frac{\partial(puE)}{\partial x} + \frac{\partial(pvE)}{\partial y} + \frac{\partial(pwE)}{\partial z} = \frac{\partial(u\sigma_{xx} + v\tau_{xy} + w\tau_{xz})}{\partial x} + \frac{\partial(v\sigma_{yy} + u\tau_{yx} + w\tau_{yz})}{\partial y} + \frac{\partial(w\sigma_{zz} + v\tau_{zy} + u\tau_{zx})}{\partial z} + \frac{\partial}{\partial x} \left( k \frac{\partial T}{\partial x} \right) + \frac{\partial}{\partial y} \left( k \frac{\partial T}{\partial y} \right) + \frac{\partial}{\partial z} \left( k \frac{\partial T}{\partial z} \right) \quad (3)$$

Model is divided into meshes and the above equations are solved for each mesh structure. Thus, velocity, pressure and temperature values of the flow behavior are determined.

## 2.2. Turbulence Models

There are three basic turbulence approaches for the solution of turbulent flow in a fluid stream. These are Direct Numerical Simulation (DNS), Large Eddy Simulation (LES) and Reynolds-Averaged Navier-Stokes (RANS) approaches. In the DNS approach, a large computational capacity is required for the solution of Navier-Stokes equations. The required computational capacity can be reduced in the LES approach. The LES approach separates the turbulence in turbulent flow into two components using separators. Although the LES approach is more efficient than DNS when the computational time is considered, in large-scale numerical applications the LES approach can be seen as time-consuming. In the RANS approach, some turbulence closing equations are added to the Navier-Stokes equations. Residuals from the mean value of turbulence stresses are included in the solution by adding them to the Navier-Stokes equations as additional turbulence stresses. It is an appropriate approach to solve numerical applications with high Reynolds numbers within low computer capacity [10]. Turbulence models in the Ansys Fluent software are classified as follows [11] [12] [13]:

- LES Models:
  1. Detached Eddy Simulation
  2. Large Eddy Simulation
- RANS models:
  1. One-Equation Model
  2. Spalart-Allmaras
  3. Two-Equation Models
  4. Standard k-ε
  5. RNG k-ε
  6. Realizable k-ε
  7. Standard k-ω
  8. SST k-ω
  9. 4-Equation v2f
  10. Reynolds Stress Model
  11. k-kl-ω Transition Model
  12. SST Transition Model

### 3. WIND PRESSURE CALCULATION ACCORDING TO EUROCODE-1

In this section, principles and calculation steps in the Eurocode-1 will be given to determine wind pressure in the external surfaces of the rectangular building. Then, details in the determination of the 15° degree duo-pitched roof building are explained when considering terrain category-0. In the same manner, for all terrain conditions, the results of external surface pressure will be submitted by considering all of the building types.

Here, the external wall pressures according to the five different terrain categories in Eurocode-1 are given in Table 1. For each terrain categories, four different buildings having a rectangular plan and duo-pitched roofs with angles of 15°, 30°, 45° and 60° are considered to calculate wind pressure acting external surfaces of the buildings in Figure 1.

#### 3.1. Principles to Determine Wind Pressure in Eurocode-1

The determination of building external surface pressure according to Eurocode-1 will be explained below. First of all, it is necessary to know the fundamental value of the basic wind velocity which is suitable for the location where the building is located. Thereafter as finding the basic wind velocity, mean wind velocity, standard deviation of the turbulence, turbulence intensity and peak velocity pressure which are terms linked to each other respectively; multiplication of the peak velocity pressure by the given pressure coefficient of a zone of a building type within the standard is determined as the external wall wind pressure of the zone.

“The fundamental value of the basic wind velocity ( $V_{b,0}$ ) is the characteristic 10 minutes mean wind velocity, irrespective of wind direction and time of year, at 10 m above ground level in open country terrain with low vegetation such as grass and isolated obstacles with separations of at least 20 obstacle heights” [1].  $V_{b,0} = 28$  m/s is taken as the basic value of the main wind velocity in this study.

##### Basic Wind Velocity ( $V_b$ ):

Basic wind velocity depends on the fundamental value of the basic wind velocity, the directional factor ( $c_{dir}$ ), seasonal factor ( $c_{season}$ ), and probability factor ( $C_{prop}$ ). Formulation for the basic wind velocity is given in Equation 4.

$$V_b = c_{dir} * c_{season} * V_{b,0} * (C_{prop}) \quad (4)$$

The recommended value for factors of the seasonal and the direction in Equation 4 is 1.0. (Also see EN 1991-1-6.)

The relation to the probability factor of Equation 4 is given in Equation 5.

$$C_{prob} = \left( \frac{1-K*\ln(-\ln(1-p))}{1-K*\ln(-\ln(0,98))} \right)^n \quad (5)$$

The descriptions and the values of the parameters in Equation 5 are given below. P is the probability factor; K is the shape parameter depending on the coefficient of variation of the extreme-value distribution; n is the exponent. Values recommended for the parameters in Eurocode-1 are; P = 0.02, K = 0.2, n = 0.5. (See also EN 1991-1-6.)

##### The Mean Wind Velocity ( $V_m$ ):

Mean wind velocity depends on the orography factor ( $c_o$ ), the roughness factor ( $c_r$ ), and the basic wind velocity. Formulation of the mean wind velocity is given in Equation 6.

$$V_m(z) = c_r(z) * c_o(z) * V_b \quad (6)$$

If the terrain orography can be ignored, the recommended value for the orographic factor in Equation 6 is 1.0. (see Section 4.3.3 in Eurocode-1.)

The roughness factor found in Equation 6 depends on the terrain factor ( $k_r$ ) and the height of the highest point of the structure including the roof (z). Moreover, it bases on the roughness

length ( $z_0$ ) and the minimum height ( $z_{min}$ ) that are given by each different terrain category in Table 1. Formulation for the roughness factor is given in Equation 7.

$$c_r(z) = k_r * \ln\left(\frac{z}{z_0}\right) \quad z_{min} \leq z \leq z_{max}$$

$$c_r(z) = c_r(z_{enküçük}) \quad z \leq z_{min} \quad (7)$$

Equation 8 is valid when the height of the buildings does not exceed the maximum height ( $z_{max}$ ) that is 200 m. The terrain factor depends on the topography length given in Table 1 for each different terrain category and the roughness length ( $z_{0,2}$ ) of the terrain category 2. Formulation for the terrain factor is given in Equation 8.

$$k_r = 0.19 * \left(\frac{z_0}{z_{0,11}}\right)^{0.07} \quad (8)$$

**The Standard Deviation of the Turbulence ( $\sigma_v$ ) and Turbulence Intensity ( $I_v(z)$ ):**

The standard deviation of the turbulence ( $\sigma_v$ ) depends on the terrain factor, basic wind velocity and the turbulence factor ( $k_t$ ). Formulation for the standard deviation of turbulence is given in Equation 9.

$$\sigma_v = k_r * V_b * k_t \quad (9)$$

The recommended value for the turbulence factor in Equation 9 is 1.0. The wind turbulence intensity is calculated depending on the standard deviation of the turbulence and the mean wind velocity. Formulation for wind turbulence intensity is given in Equation 10.

$$I_v(z) = \frac{\sigma_v}{V_m(z)} = \frac{k_t}{c_o(z) * \ln\left(\frac{z}{z_0}\right)} \quad z_{min} \leq z \leq z_{max} \quad (10)$$

$$I_v(z) = I_v(z_{min}) \quad z < z_{min}$$

**The Peak Velocity Pressure ( $q_p(z)$ ) :**

The peak velocity pressure is obtained depending on the mean wind velocity, the air density ( $p$ ) and turbulence intensity. Formulation for peak velocity pressure is given in Equation 11.

$$q_p(z) = [1 + 7 * I_v(z)] * \frac{1}{2} * p * V_m^2(z) \quad (11)$$

where air density ( $p$ ) is taken as 1.25 kg/m<sup>3</sup>.

**The Wind Pressure Acting on the External Surfaces, ( $W_e$ ):**

The wind pressure acting on the external surfaces is obtained by multiplying the peak pressure velocity with the pressure coefficient for the external pressure ( $c_{pe}$ ). Formulation for the wind pressure acting on the external surfaces is given in Equation 12. The external pressure coefficient in each external surface is given in Eurocode-1. The external pressure coefficient for the vertical walls of rectangular plan buildings within is given in EN 1991-1-4 Table 7.1, while the external pressure coefficient for duo-pitched roofs is given in EN 1991-1-4 Table 7.4.a.

$$W_e = q_p(z) * c_{pe} \quad (12)$$

**3.2. A Numerical Example Case Covering A Terrain Category and A Duo-pitched Roof**

Details of wind pressure calculations for a building given in Figure 1 are illustrated in Figure 2. In this illustration, the building has a rectangular plan and a roof pitch of 15° for terrain category-0. In Figure 2 the external surface wind pressure is determined considering the peak velocity pressure for the terrain category-0 with a 15° degree duo-pitched roof using Equation 1-8 in order.

**Table 1.** Terrain categories

Terrain Category	z <sub>0</sub> (m)	Z <sub>min</sub> (m)
0-) Sea or coastal area exposed to the open sea	0.003	1
1-) Lakes or flat and horizontal area with negligible vegetation and without obstacles	0.01	1
2-) Area with low vegetation such as grass and isolated obstacles (trees, buildings) with separations of at least 20 obstacle heights	0.05	2
3-) Area with a regular cover of vegetation or buildings or with isolated obstacles with separations of maximum 20 obstacle heights (such as villages, suburban terrain, permanent forest)	0.3	5
4-) Area in which at least 15 % of the surface is covered with buildings and their average height exceeds 15 m	1.0	10

Roughness Length z <sub>0</sub>	=	0.003	m	(EN 1991-1-4 Table4.1)
Minimum Height z <sub>min</sub>	=	1.0	m	(EN 1991-1-4 Table4.1)
Terrain Factor	$k_T = 0.19 \times \left(\frac{z_0}{z_{0,II}}\right)^{0.07}$	=	0.156	(EN 1991-1-4 Equation 4.5)
Roughness Factor	$c_i(z) = k_T \times \ln\left(\frac{z}{z_0}\right)$	=	1.244	(EN 1991-1-4 Equation 4.4)
Orography Factor c <sub>o</sub> (z)	=	1		(EN 1991-1-4_4.3.1)
Turbulence Intensity I <sub>v</sub>	$I_v = \frac{k_T}{c_o(z) \times \ln(z/z_0)}$	=	0.125	(EN 1991-1-4 Equation 4.7)
Peak Velocity Pressure q <sub>p</sub> (z)				(EN 1991-1-4 Equation 4.8)
	$q_p(z) = \left[1 + \frac{7k_T}{c_o(z) \times \ln(z/z_0)}\right] \times \frac{1}{2} \times \rho \times (v_b \times c_r \times c_o)^2$			; p = 1.25 kg/m <sup>3</sup>
		q <sub>p(z)</sub>	=	1424 N/m <sup>2</sup>

**Figure 2.** The result of peak velocity pressure

The pressure coefficients of the building that are perpendicular to the direction of blowing wind are given for front and rear facade in Figure 3. This front and rear facade correspond to zones D and E in Figure 3, respectively.

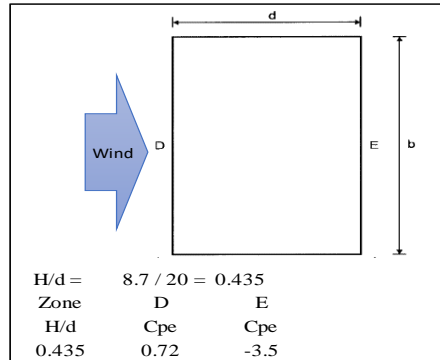


Figure 3. Pressure coefficients for vertical walls of a building

The pressure coefficients of roof surfaces are given for each roof zone in Figure 4. Front roof surface is divided into two zones such as zone G and zone H as well as rear roof surface such as zone J and zone I in the direction of the wind. The calculated external pressures of the zones are given in Figure 5.

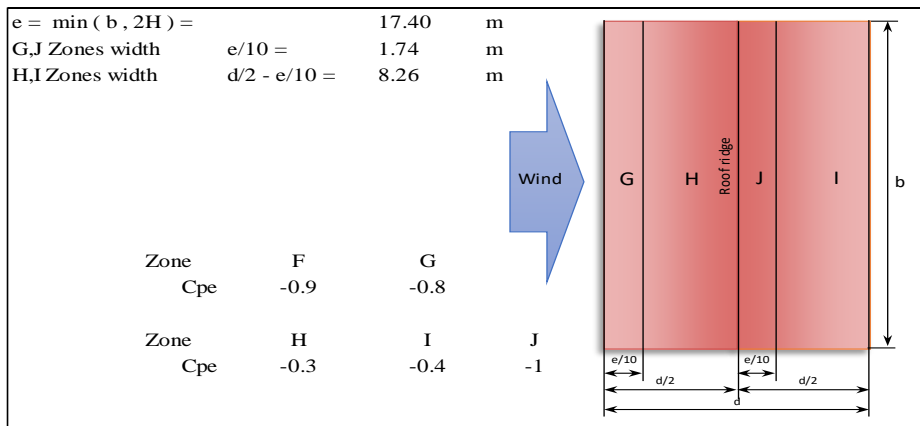


Figure 4. Pressure coefficients for roof surfaces

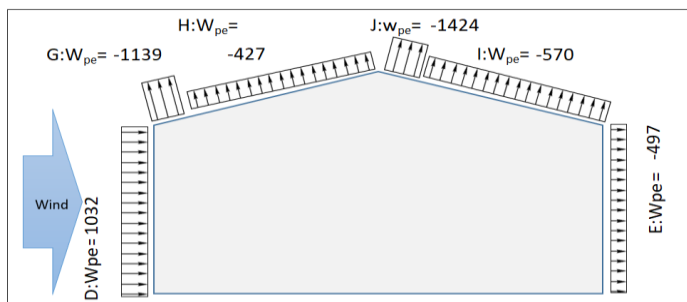


Figure 5. Results of the external pressures ( $Pa = N/m^2$ ) in 15° degrees duo pitched roof building for terrain category-0



According to the other terrain categories in Eurocode-1, the results of external surface pressure for the building will be given in the following subsection. Moreover, the results of external surface pressure for the other buildings having a duo-pitched roof in Figure 1 will be submitted in the following subsection according to all of the terrain categories in Eurocode-1.

### 3.3. Numerical Results for Example Cases Covering All of Terrain Category and Duo-pitched Roofs

According to Eurocode-1, pressure coefficients for external surface pressure in the zones of the buildings in Figure 1 are presented in Table 2.

**Table 2.** Pressure coefficients for external surface pressure ( $C_{pe}$ )

Structure Type	Structure Surface Zones					
	D	G	H	J	I	E
15° Degree Duo-pitched Roof	0.72	-0.8	-0.3	-1	-0.4	-0.35
30° Degree Duo-pitched Roof	0.75	-0.5	-0.2	-0.5	-0.4	-0.39
45° Degree Duo-pitched Roof	0.77	0.7	0.6	-0.3	-0.2	-0.45
60° Degree Duo-pitched Roof	0.80	0.7	0.7	-0.3	-0.2	-0.50

The peak velocity pressures are attained considering each building in Figure 1 within all of the terrain categories in Eurocode-1. When multiplying the peak velocity pressures with the pressure coefficients, external pressures are achieved in each zone of the buildings having 15°, 30°, 45°, and 60° degrees duo-pitched roofs in Table 3, Table 4, Table 5 and Table 6, respectively.

**Table 3.** Results of external wall pressure in a building with 15° degree duo-pitched roof ( $Pa = N/m^2$ )

ZONE	D	G	H	J	I	E
TERRAIN CATEGORY-0	1032	-1139	-427	-1424	-570	-497
TERRAIN CATEGORY-1	954	-1053	-395	-1316	-526	-460
TERRAIN CATEGORY-2	804	-888	-333	-1110	-444	-388
TERRAIN CATEGORY-3	575	-635	-238	-794	-317	-277
TERRAIN CATEGORY-4	418	-461	-173	-576	-231	-201

**Table 4.** Results of external wall pressure in a building with a 30° degree duo-pitched roof ( $Pa = N/m^2$ )

ZONE	D	G	H	J	I	E
TERRAIN CATEGORY-0	1125	-755	-302	-755	-604	-590
TERRAIN CATEGORY-1	1048	-703	-281	-703	-562	-549
TERRAIN CATEGORY-2	897	-602	-241	-602	-482	-470
TERRAIN CATEGORY-3	664	-446	-178	-446	-356	-348
TERRAIN CATEGORY-4	469	-315	-126	-315	-252	-246

**Table 5.** Results of external wall pressure in a building with a 45° degree duo-pitched roof (Pa = N/m<sup>2</sup>)

ZONE	D	G	H	J	I	E
TERRAIN CATEGORY-0	1233	1117	957	-479	-319	-712
TERRAIN CATEGORY-1	1158	1049	899	-449	-300	-669
TERRAIN CATEGORY-2	1008	912,1	782	-391	-261	-582
TERRAIN CATEGORY-3	767	694	595	-298	-198	-443
TERRAIN CATEGORY-4	564	510	437	-219	-146	-326

**Table 6.** Results of external wall pressure in a building with a 60° degree duo-pitched roof (Pa = N/m<sup>2</sup>)

ZONE	D	G	H	J	I	E
TERRAIN CATEGORY-0	1365	1194	1194	-512	-341	-867
TERRAIN CATEGORY-1	1293	1131	1131	-485	-323	-821
TERRAIN CATEGORY-2	1143	1000	1000	-429	-286	-726
TERRAIN CATEGORY-3	899	787	787	-337	-225	-571
TERRAIN CATEGORY-4	688	602	602	-258	-172	-437

#### 4. EXTERNAL PRESSURE ACCORDING to TS 498

In this section, the results of the external pressure of the buildings in Figure 1 are obtained according to TS 498. In TS 498, peak velocity pressure (q) is determined using the air density (p), wind velocity (V) and the gravitational acceleration (g) as in Equation 13.

$$q = p \frac{v^2}{2g} \tag{13}$$

The air density (p) is 1, 25 kg/m<sup>3</sup> in Equation 10. Here, the peak velocity pressure is arranged with respect to the height from the ground. Then, peak velocity pressure is driven by Equation 10. Table 7 presents the peak velocity pressures with wind velocities at the specified height intervals.

**Table 7.** Peak velocity pressure

Height From The Ground (m)	Wind Velocity -V (m/s)	Velocity Pressure-q (kN/m <sup>2</sup> )
0~8	28	0.5
9~20	36	0.8
21~100	42	1.1
>100	46	1.3

The building surface areas and the pressure coefficients (c<sub>p</sub>) to be considered according to TS 498 are given in Figure 6. Relevant external wall pressure coefficients are taken from Figure 1 of TS 498. According to TS 498, there are no different areas on the roof wall surfaces as in Eurocode-1. Eurocode-1 has two different zones on the roof surfaces, as explained in section 3.

External wall pressure (W) is obtained by multiplying the velocity pressures given in Table 7 with the pressure coefficients given in Figure 6. Formulation for the external wall pressure is given in Equation 14.

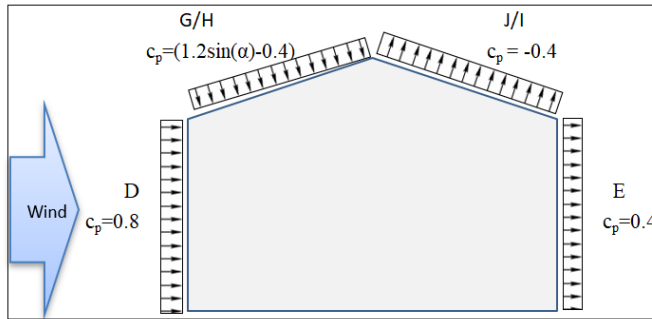


**Figure 6.** TS 498 building surfaces and pressure coefficients

$$W = c_p * q \tag{14}$$

For building surface areas given in Figure 6 whose external wall pressure results are given in Table 8 by having calculated according to TS 498 principles, the four different buildings whose geometrical structures are given in Figure 1.

**Table 8.** TS 498 external wall pressure result (Pa = N/m<sup>2</sup>)

ZONE	D	G-H	J-I	E
15° Degree Duo-pitched Roof	392	-72.43	-324	-196
30° Degree Duo-pitched Roof	392	162.00	-324	-196
45° Degree Duo-pitched Roof	392	363.21	-324	-196
60° Degree Duo-pitched Roof	392	517.78	-324	-196

There is no calculation based on the different terrain categories as in Eurocode-1 in the TS 498 standard. Therefore, there is only one external wall pressure result for each structure in Table 8.

## 5. ANALYSES of COMPUTATIONAL FLUID DYNAMIC MODELS

In this section, pre-process stage of computational fluid dynamic models (CFD models) such as flow field and boundary conditions, mesh structure, analysis option, velocity function of the inlet is defined, analyses of CFD are carried out, and the results of external wall pressure are submitted below.

### 5.1. Flow Field and Boundary Conditions

While wall boundary is assigned to the surfaces of the building, boundary conditions such as velocity inlet and pressure outlet are defined in the analysis with a velocity profile and free pressure surface, respectively. The wall boundary engages that fluid velocity is zero on the building surfaces. These boundary regions are shown in Figure 7. The velocity profile is a function which is associated with the elevation and the ground boundary condition according to Eurocode-1. Information about the velocity function will be given in Section 5.4. Moreover, the symmetric boundary condition is assigned to the ground boundary and top boundary since the velocity function includes ground friction status (see Figure 10).

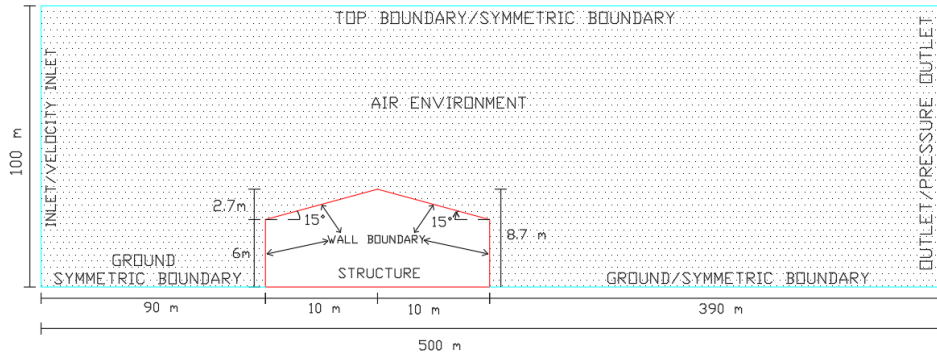


**Figure 7.** Dimensions and boundary conditions of building flow field

The environment surrounding the building is defined as air. The flow field in Figure 7 is considered as same in the analysis of all types of buildings in Figure 1. For example, the geometry of the building with a roof pitch angles of  $15^\circ$  is used in Figure 7.

In Figure 7, the shortest distance of the building boundary to the inlet of the flow field is approximately five times of the building width, the shortest distance of the building boundary to the outlet of the flow field is approximately twenty times of the building width, and the shortest distance between the upper boundary of the flow field and upper point of the building boundary is determined as approximately five times of the building height. At the literature, the dimensions mentioned above are used to determine a flow field [6] [14] [15].

## 5.2. Mesh Structure

In order to get a mesh giving a converged result, the key point is to make fairly fine the mesh. To create so massive mesh is so expensive while considering solution time of the analysis. Because of that, a strategy while creating a mesh is followed. According to the strategy, the mesh is made fine when getting near to the building boundary. Therefore, the coarse mesh is considered in the far field from the building boundary. To follow the strategy achieves to get results of the velocity and pressure with high accuracy. The model and mesh of the flow field are shown in Figure 8. Figure 8 covers (a) view of model of the flow field, (b) view of a mesh of the model, (c) near-field view of the mesh, and (d) near-field view of the mesh close to the building boundary.

In the aerodynamic analysis, the depth of the region of the flow field near the wall is an important condition that should not be neglected. Size of the nearest mesh in the normal direction of the boundary surfaces is determined according to the depth of the region of the flow field near the building boundary. The size should be adequate thin to model the viscous sublayer near the building boundary. In the calculation of the size, Reynolds number, characteristic length, and fluid parameters are used. The graph containing the Universal Wall Law which is used to determine the mesh depth is given in Figure 9 [11] [12] [13].

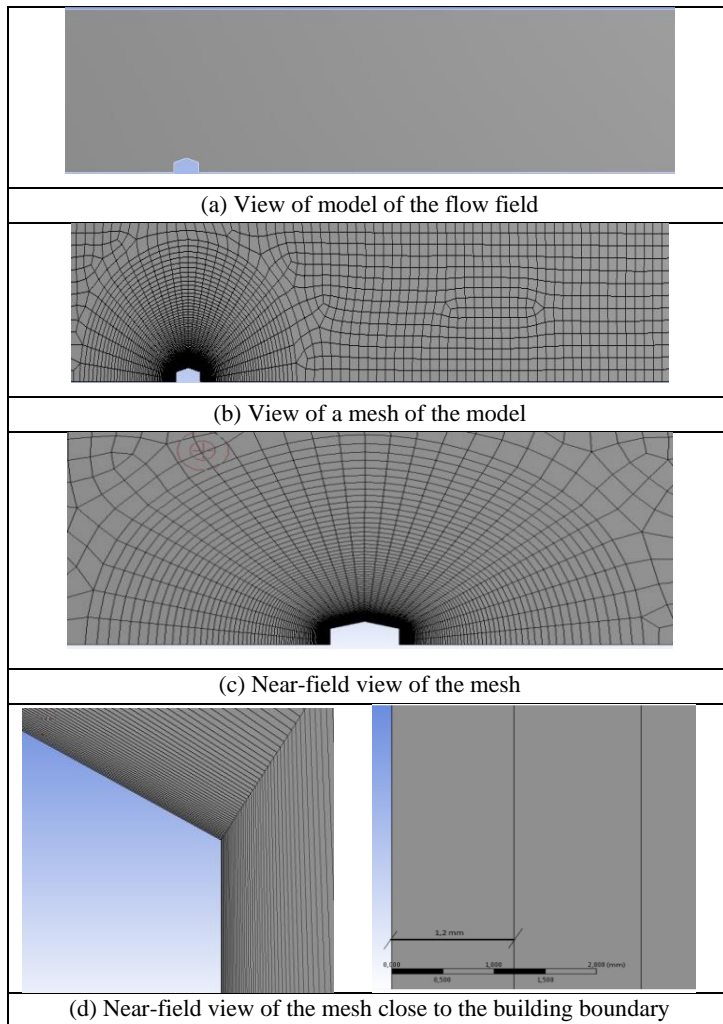


**Figure 8.** Model and mesh structure

The dimensionless velocity ( $u^+$ ) and the depth coefficient ( $y^+$ ) are parameters related to the Universal Wall Law. Depth Coefficient depends on the depth, shear stress velocity ( $u_\tau$ ) of the fluid and the kinematic viscosity ( $\nu$ ) of the air. The dimensionless velocity depends on the fluid velocity ( $u$ ) and the shear stress velocity. Formulation for the depth coefficient and the dimensionless velocity are given in Equation 15.

$$y^+ = \frac{y u_\tau}{\nu} \quad u^+ = \frac{u}{u_\tau} \quad (15)$$

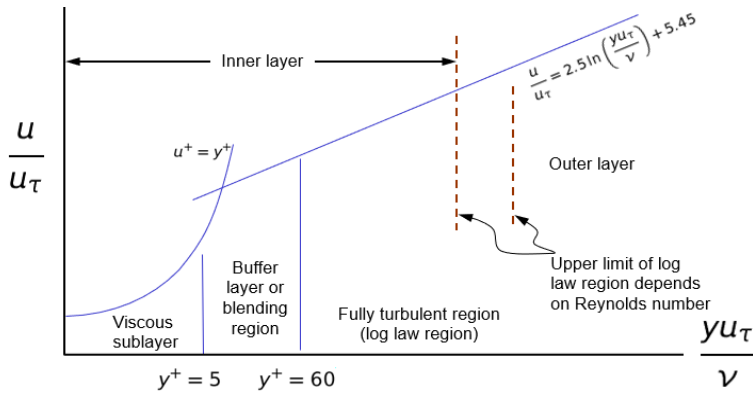


**Figure 9.** Universal Wall Law

Equation 15 is given for explanation of the coefficients which are chosen as value and determined at the last paragraph of this subsection. The depth depends on the depth coefficient ( $y^+$ ), the shear stress velocity, the kinematic viscosity of air. Formulation for the depth is given in Equation 16.

$$y = \frac{y^+ * \nu}{u_\tau} \tag{16}$$

Where shear stress velocity depends on the wall shear stress and air density. Formulation for the shear stress velocity is given in Equation 17.

$$u_\tau = \sqrt{\frac{Z_w}{\rho}} \tag{17}$$

Where wall shear stress ( $Z_w$ ) depends on the surface roughness ( $C_f$ ), air density, and fluid velocity. Formulation for the wall shear stress is given in Equation 18.

$$Z_w = 0.5 * C_f * \rho * u^2 \tag{18}$$

where the surface roughness is the parameter given in Equation 19, which depends on the Reynolds number.

$$C_f = 0.058 * (Re_L)^{-0.2} \tag{19}$$

Where Reynolds number ( $Re_L$ ) depends on air density, the kinematic viscosity, the fluid velocity and the characteristic length (width of the building in this study) in the direction of the wind ( $L$ ). Formulation for the Reynolds number is given in Equation 20.

$$Re_L = \frac{\rho u L}{\mu} \tag{20}$$

In this study, some parameters in the models are taken as follows; fluid velocity,  $u = 28$  m/s; air density,  $\rho = 1.25$  kg/m<sup>3</sup>; kinematic viscosity of air,  $\mu = 1.8 \times 10^{-5}$  kg/ms; the width of building in the direction of the effect of the wind,  $L = 20$  m, the depth coefficient,  $y^+ = 70$ , the depth  $y = 0.0012$  m. The depth coefficient in the literature is in the range of 30-300 so that SKE, RKE, RNG turbulence models and "Scalable Wall Functions" wall approaches can be used in the range of depth [11] [12] [13].

### 5.3. Analysis Options

The turbulence model used in the study is as "k -  $\epsilon$  Realizable". Wall approach in the turbulence model was chosen as "Scalable Wall function." [5] [7] [8] [14] [16]. "Simple

algorithm" is chosen in velocity pressure relations for the solution method. The "Second-Order Upwind Scheme" is used for solving between variable mesh types. The "Standard" method is used interpolation schemes for calculating cell-face pressures when using the pressure-based solver. Moreover, that normalized residuals are to be less than an order of  $10^{-6}$  is considered as convergence criterion of solutions for the results of continuity equation, momentum equation, and k and epsilon equation.

### 5.4. Velocity Function

Velocity function is determined with Equation 21 that is created by the combination of Equation 1, Equation 2, Equation 3, Equation 4, and Equation 5.

$$V_m = 0.19 * (z_0/z_{0,11})^{0.07} * V_b * \ln(z/z_0) \tag{21}$$

In this study, base velocity is chosen as 28 m/s and terrain categories are considered as in Table 9 and Figure 10 where velocity function is obtained with respect to terrain category.

**Table 9.** Velocity function with respect to terrain category

Terrain Category	$z_{0,2}$	$z_0$	$V_b$ (m/s)	Equation (21)
0	0.05	0.003	28	$4.37 * \ln(z/0,003)$
1	0.05	0.01	28	$4.75 * \ln(z/0,01)$
2	0.05	0.05	28	$5.32 * \ln(z/0,05)$
3	0.05	0.3	28	$6.03 * \ln(z/0,3)$
4	0.05	1	28	$6.56 * \ln(z/1,0)$

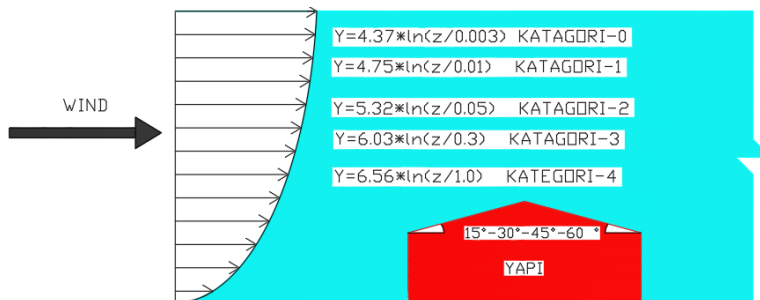


**Figure 10.** Wind velocity function on the flow field

The depth of the flow field is 100 m and so depth (z) in velocity profile is determined in analysis depending on the range of 0-100 m. As an example, velocity function for terrain category-2 is shown in Figure 11. Velocity functions shown in Table 9 has been presented as velocity profile [17] in the models.

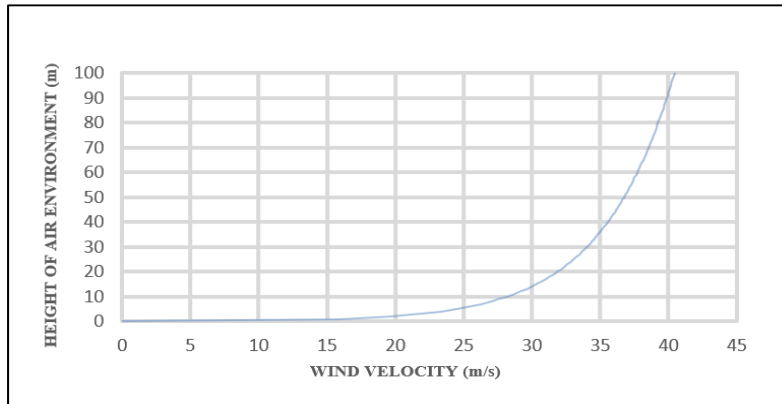
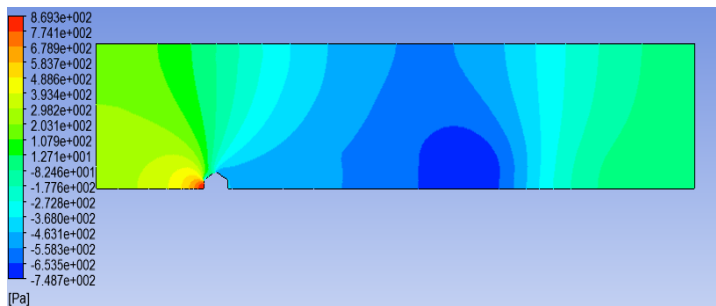


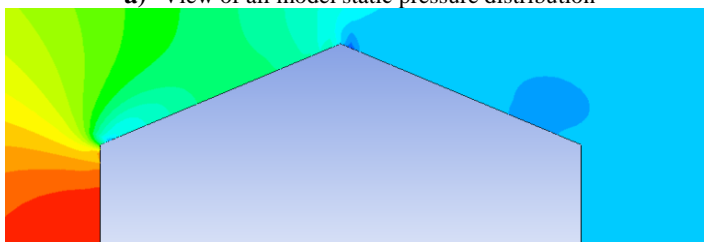
**Figure 11.** Velocity function of terrain category-2

### 5.5. Analysis Results

Distributions of pressure and velocity regarding the analysis results of the building with 15° degree duo-pitched roof, while considering terrain category-0, are shown in Figure 12 and Figure 13, respectively.



**a)** View of all model static pressure distribution



**b)** Near-field view of the building static pressure distribution

**Figure 12.** Static pressure distribution ( $\text{Pa} = \text{N/m}^2$ )

After solutions of the models, the results of the external wall pressure are given by considering the buildings with a roof pitch angles of 15°- 30°- 45°- 60° with respect to the five different terrain categories in Table 10, Table 11, Table 12 and Table 13, respectively.



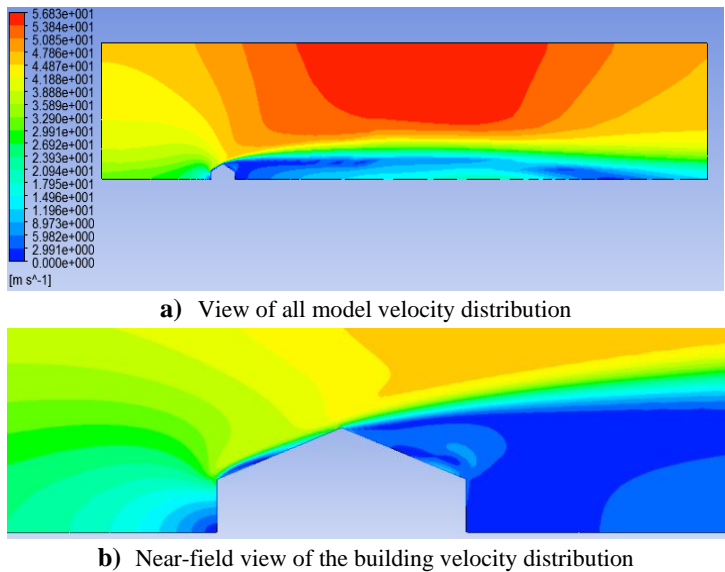


Figure 13. Velocity distribution on the global range (m/s)

Table 10. Results of external pressure in a building with 15°degree duo-pitched roof (Pa = N/m<sup>2</sup>)

ZONE	D	G	H	J	I	E
TERRAIN CATEGORY-0	712	-1730	-995	-1340	-717	-465
TERRAIN CATEGORY-1	588	-1600	-750	-1170	-620	-405
TERRAIN CATEGORY-2	407	-1145	-605	-920	-503	-295
TERRAIN CATEGORY-3	200	-570	-345	-500	-270	-160
TERRAIN CATEGORY-4	165	-380	-187	-420	-187	-145

Table 11. Results of external pressure in a building with 30°degree duo-pitched roof (Pa = N/m<sup>2</sup>)

ZONE	D	G	H	J	I	E
TERRAIN CATEGORY-0	869	-586	-263	-670	-586	-505
TERRAIN CATEGORY-1	729	-280	-250	-615	-480	-413
TERRAIN CATEGORY-2	511	-312	-215	-458	-410	-312
TERRAIN CATEGORY-3	258	-170	-116	-276	-248	-195
TERRAIN CATEGORY-4	200	-110	-95	-220	-210	-145

Table 12. Results of external pressure in a building with 45°degree duo-pitched roof (Pa = N/m<sup>2</sup>)

ZONE	D	G	H	J	I	E
TERRAIN CATEGORY-0	1119	783	780	-805	-805	-680
TERRAIN CATEGORY-1	1041	736	730	-775	-775	-637
TERRAIN CATEGORY-2	775	410	410	-585	-495	-480
TERRAIN CATEGORY-3	465	305	305	-314	-275	-318
TERRAIN CATEGORY-4	390	285	285	-225	-205	-250

**Table 13.** Results of external pressure in a building with 60°degree duo-pitched roof (Pa = N/m<sup>2</sup>)

ZONE	D	G	H	J	I	E
TERRAIN CATEGORY-0	1170	817	817	-1270	-915	-576
TERRAIN CATEGORY-1	1000	698	698	-1115	-834	-528
TERRAIN CATEGORY-2	735	497	497	-905	-670	-441
TERRAIN CATEGORY-3	483	340	340	-570	-515	-372
TERRAIN CATEGORY-4	265	175	175	-430	-250	-175

## 6. DISCUSSIONS

Table 14, Table 15, Table 16 and Table 17 that contain proportional expressions is generated by dividing the results obtained from Eurocode-1 (see Table 3-4-5-6) to the results obtained from the CFD analyses (see Table 10-11-12-13).

**Table 14.** Results of external pressure in a building with 15°degree duo-pitched roof (Pa = N/m<sup>2</sup>)

ZONE	D	G	H	J	I	E
TERRAIN CATEGORY-0	1.45	0.66	0.43	1.06	0.79	1.07
TERRAIN CATEGORY-1	1.62	0.66	0.53	1.12	0.85	1.14
TERRAIN CATEGORY-2	1.98	0.78	0.55	1.21	0.88	1.31
TERRAIN CATEGORY-3	2.88	1.11	0.69	1.59	1.18	1.73
TERRAIN CATEGORY-4	2.53	1.21	0.92	1.37	1.23	1.39

**Table 15.** Results of external pressure in a building with 30°degree duo-pitched roof (Pa = N/m<sup>2</sup>)

ZONE	D	G	H	J	I	E
TERRAIN CATEGORY-0	1.29	1.29	1.15	1.13	1.03	1.17
TERRAIN CATEGORY-1	1.44	2.51	1.12	1.14	1.17	1.33
TERRAIN CATEGORY-2	1.76	1.93	1.12	1.31	1.17	1.51
TERRAIN CATEGORY-3	2.57	2.62	1.54	1.61	1.44	1.79
TERRAIN CATEGORY-4	2.34	2.86	1.32	1.43	1.20	1.69

**Table 16.** Results of external pressure in a building with 45°degree duo-pitched roof (Pa = N/m<sup>2</sup>)

ZONE	D	G	H	J	I	E
TERRAIN CATEGORY-0	1.10	1.43	1.23	0.59	0.40	1.05
TERRAIN CATEGORY-1	1.11	1.42	1.23	0.58	0.39	1.05
TERRAIN CATEGORY-2	1.30	2.22	1.91	0.67	0.53	1.21
TERRAIN CATEGORY-3	1.65	2.28	1.95	0.95	0.72	1.39
TERRAIN CATEGORY-4	1.45	1.79	1.53	0.97	0.71	1.30

**Table 17.** Results of external pressure in a building with 60°degree duo-pitched roof (Pa = N/m<sup>2</sup>)

ZONE	D	G	H	J	I	E
TERRAIN CATEGORY-0	1.17	1.46	1.46	0.40	0.37	1.51
TERRAIN CATEGORY-1	1.29	1.62	1.62	0.43	0.39	1.56
TERRAIN CATEGORY-2	1.56	2.01	2.01	0.47	0.43	1.65
TERRAIN CATEGORY-3	1.86	2.31	2.31	0.59	0.44	1.54
TERRAIN CATEGORY-4	2.60	3.44	3.44	0.60	0.69	2.50

Assessments of results of TS 498, which is kind of external wall pressure, are going to be done below while comparing with results of external wall pressure for Eurocode-1 and CFD Analyses results.

**Comparison of Details of TS 498 and Eurocode-1;**

- TS 498 does not contain information on the change in pressure values concerning different terrain categories as in Eurocode-1. In Eurocode-1, five different values of external wall pressure can be determined with regard to terrain categories.
- TS 498 has velocity values that vary according to certain altitude ranges. Depending on this velocity, different velocity pressures are available for different altitude ranges. Moreover, the intensity of any turbulence does not affect wind velocity pressure when considering TS 498. In Eurocode-1, however, basic wind velocity according to the highest top of the building and mean wind velocity based on terrain category type. Depending on the mean wind velocity and the value of the turbulence intensity, peak velocity pressure is determined. Due to the before mentioned conditions, the wind velocity pressure used in TS 498 is being lower than the peak velocity pressure in Eurocode-1.
- In TS 498 and Eurocode-1, wind velocity pressures are converted to external wall pressures of the relevant surfaces of a building by multiplying the pressure coefficients that are given in the standards.

**Relative assessments of the results of TS 498 and EUROCODE-1 (See Table 8 /Table 3-4-5-6);**

- Positive pressure (pressure perpendicular to the surface) is formed for zone D when the results of the two standards are considered. In addition, the values found for TS 498 for this zone are being lower than those for all the terrain categories in Eurocode-1.
- Negative pressure (tensile perpendicular to the surface) is formed for zone E when the results of the two standards are considered. In addition, the values found for TS 498 for this zone are being lower than those for all the terrain categories in Eurocode-1.
- In TS 498, there are no turbulence-induced different zones occurring on the roof surfaces. In G-H roof surface areas (see Figure 4) in TS 498, positive pressure occurs on the roof surfaces of buildings with a roof pitch angle up to 23° negative pressure on the roof surfaces of buildings with a roof pitch angle more than 23°. However, there is always a negative pressure in the J-I surface area (see Figure 4).

In Eurocode-1 observing the four different structures considered for G and H roof surface areas, negative pressure is generated on 15° and 30° pitched roofs and positive pressure is generated on 45° and 60° pitched roofs of buildings. However, there is always a negative pressure in the J and I surface areas. In general, the results of TS 498 in roof surface areas are being lower than those of Eurocode-1.

**Relative assessments of the results of CFD analyses and EUROCODE-1 (See Table 14-15-16-17);**

Whereas the wind function used for the CFD analyzes and Eurocode-1 are same, the turbulence intensities affecting the results do not match with each other. Eurocode-1 takes into consideration turbulence with Equation 7 and Equation 8. However, Navier-Stokes equations added with turbulence closure equations are used to determine the turbulence severity depending on the turbulence model in a CFD analysis [11] [12] [13]. This seems to be the cause of some differences between the results of CFD analyses and Eurocode-1.

- Positive pressure has occurred in Zone D in both of the results of CFD analyses and Eurocode-1. It is seen that the results of Eurocode-1 within the range of 1.1 and 2.88 times are greater than the results of CFD analyses when considering five different terrain categories. Eurocode-1 finds the pressure value of each zone depending on the wind velocity at the highest top of the building. However, in the CFD analyses, the wind pressure in each point is calculated depending on the wind velocity in that point.

- Negative pressure has occurred in Zone E in both of the results of CFD analyses and Eurocode-1. It is seen that the results of Eurocode-1 within the range of 1.05 and 2.5 times are greater than the results of CFD analyses when considering five different terrain categories.

- Negative pressure in G Area of 15° and 30° pitched roof buildings has been formed in both of the results of CFD analyses and Eurocode-1. It is seen for 30° pitched roof building that the results of Eurocode-1 within the range of 1.29 and 2.86 times are greater than the results of CFD analyses when considering five different terrain categories. It is seen for 15° pitched roof building that the results of Eurocode-1 1.20 times are greater than the results of CFD analyses when considering most terrain categories. Since the turbulence effect is high in the analysis at the sharp corners of the buildings, the results of Eurocode-1 can be lower than those of the CFD analyses. Similar results are available in the literature [6]. Positive pressure in surfaces of 45° and 60° pitched roof buildings has been formed in both of the results of CFD analyses and Eurocode-1. It is seen for 30° pitched roof building that the results of Eurocode-1 within the ratio of 1.41 and 3.44 times are greater than the results of CFD analyses when considering five different terrain categories.

- Negative pressure in H Area of 15° and 30° pitched roof buildings has been formed in both of the results of CFD analyses and Eurocode-1. It is seen for 30° pitched roof building that the results of Eurocode-1 within the range of 1.15 and 1.54 times are greater than the results of CFD analyses when considering five different terrain categories. The results of Eurocode-1 for 15° pitched roof building are lower than the results of CFD analyses. Since the turbulence effect is high in the analysis at the sharp corners of the buildings, the results of Eurocode-1 can be lower than those of the CFD analyses. Similar results are available in the literature [6].

Positive pressure in surfaces of 45° and 60° pitched roof buildings has been formed in both of the results of CFD analyses and Eurocode-1. It is seen for 30° pitched roof building that the results of Eurocode-1 within the ratio of 1.23 and 3.44 times are greater than the results of CFD analyses when considering five different terrain categories.

- Negative pressure in J Area of 15° and 30° pitched roof buildings has been formed in both of the results of CFD analyses and Eurocode-1. It is seen for 30° pitched roof building that the results of Eurocode-1 within the range of 1.06 and 1.61 times are greater than the results of CFD analyses when considering five different terrain categories. The results of Eurocode-1 for 45° and 60° pitched roof building are lower than the results of CFD analyses. Since the turbulence effect is high in the analysis at the sharp corners of the buildings, the results of Eurocode-1 can be lower than those of the CFD analyses. Similar results are available in the literature [6].

- Negative pressure in I Area of all buildings has occurred in both of the results of CFD analyses and Eurocode-1. It is seen for 30° pitched roof building that the results of Eurocode-1 within the range of 1.03 and 1.44 times are greater than the results of CFD analyses when

considering five different terrain categories. Except for some terrain conditions, the results of Eurocode-1 within 1.20 times are greater than the results of CFD analyses for 15° pitched roof building. However, the results of Eurocode-1 for 45° and 60° pitched roof building are lower than the results of CFD analyses. Since the turbulence effect is high in the analysis at the sharp corners of the buildings, the results of Eurocode-1 can be lower than those of the CFD analyses. Similar results are available in the literature [6].

### **Relative assessments of the results of TS 498 and CFD analyses (See Table 8 /Table 10-11-12-13);**

Relative assessments of the results of TS 498 and CFD analyses are so similar with Relative assessments of the results of TS 498 and Eurocode-1. The results of TS 498 in D and E Areas are greater than the results of CFD analyses for terrain category. However, the results of TS 498 are lower than the results of CFD analyses for the other terrain categories. Since the turbulence effect is high in the analysis at the sharp corners of the buildings, the results of TS 498 can be lower than those of the CFD analyses in the roofs of the buildings.

## **7. CONCLUSIONS**

In this study, external wall wind pressures were investigated using Eurocode-1 and TS 498 and the CFD analyses in rectangular planned buildings with 15°, 30°, 45° and 60° degrees duo-pitched roofs. The following conclusions were derived;

- In TS 498, it is seen that external wall wind pressures are not sufficient to reach the value level of the others such as Eurocode-1 and CFD analyzes.
- Additional effects such as turbulence in the corners or folded edges are considered in Eurocode-1 and the CFD analyses, but TS 498 disregards these effects.
- Turkish Standards Institute published "Eurocode-1 - Action on structures - Part 1 - 4: General actions - Wind actions" part as the " TS EN 1991-1-4 Yapılar Üzerindeki Etkiler Bölüm 1-4: Genel Etkiler – Rüzgâr Etkileri " in December 2007. Although TS 498 published in 1997 is still in force, Turkish steel design standard called as " Çelik Yapıların Tasarım, Hesap ve Yapım Dair Esaslar [18]" refers to the TS EN 1991-1-4 for the wind calculation.
- The results of Eurocode-1 are generally higher than those of CFD analyses. Since the turbulence effect is high in the analysis at the sharp corners of the buildings, the results of Eurocode-1 can be lower than those of the CFD analyses, while considering negative pressures. This can result from the turbulence models used in CFD analyses.

When comparing the results of Eurocode-1 and CFD analyses, the results are different, but negative or positive pressures seem in the same regions for both Eurocode-1 and CFD analyses.

## **REFERENCES**

- [1] Eurocode-1. (2005).Actions on Structures/General Actions, Part 1-4:Wind Actions. CEN/TC 250,Management Centre,Brussels. (TS EN 1991-1-4. (Aralık 2007). Yapılar Üzerindeki Etkiler-Bölüm 1-4: Genel Etkiler-Rüzgar Etkileri. Türk Standartları Enstitüsü, Ankara.)
- [2] TS498. (Kasım-1997). Yapı Elemanlarının Boyutlandırılmasında Alınacak Yüklerin Hesap Değeri. Türk Standartları Enstitüsü, 2.Baskı, Ankara.
- [3] İstanbul Yüksek Binalar Rüzgar Yönetmeliği. (2009). Deprem Mühendisliği Ana Bilim Dalı Kandilli Rasathanesi ve Deprem Araştırma Enstitüsü, Versiyon V, Boğaziçi Üniversitesi Çengelköy, İstanbul.
- [4] Kurç, Ö., Kayışoğlu, B., Shojafe, N., Uzol, O. (2012). Yüksek Binalarda Rüzgar Etkilerinin Rüzgar Tüneli Deneyleriyle Tespiti. İMO Teknik Dergisi,6163-6186, yazı 389.

- [5] Özmen, Y., Kaydok, T. (2015). Farklı Kesitlere Sahip Yüksek Binalar Üzerinde Rüzgar Etkisinin Sayısal İncelenmesi. *TMH Dergisi*, 488, 40-49.
- [6] Vasilios, P. F., Georgios, N. Tinas, K., Dimitrios, L. K. (06-10.07.2014). Numerical estimation of external pressure coefficients of a pitched-type roof greenhouse and comparison with Eurocode in different flow-type circumstances. *Proceedings International Conference of Agricultural Engineering, Zurich*.
- [7] Özmen, Yücel. (2006). Farklı Çatı Tiplerinde ve Eğimlerdeki Binalar Üzerinde Rüzgar Etkilerinin Deneysel ve Teorik İncelenmesi. Doktora Tezi, Karadeniz Teknik Üniversitesi, Trabzon.
- [8] Xing, F., Mohotti, D. Chauhan, K. (2018). Experimental and Numerical Study on Mean Pressure Distributions Around an Isolated Gable Roof Building with and without Openings. *Building and Environment*, 132, 30-44.
- [9] Çengel, Y. A. Cimbala, J. A. (2008). Akışkanlar Mekaniği Temelleri ve Uygulamaları. (Çeviri Editörü: Engin, T.), İzmir Güven Kitabevi, Birinci Baskı, İzmir.
- [10] Kiriççi, Volkan. (2016). Osman Gazi Köprüsüne Etkiyen Rüzgâr Yüklerinin Had Metodu ile İncelenmesi. Yüksek Lisans Tezi, Anadolu Üniversitesi, Eskişehir.
- [11] Ansys Fluent Tutorial Guide. (2013). Release 15.0, ANSYS Inc, Canonsburg, PA.
- [12] Ansys Fluent Theory Guide. (2013). Release 15.0, ANSYS Inc, Canonsburg, PA.
- [13] Ansys Fluent Lectures. (2010). Release 13.0, ANSYS Inc, Canonsburg, PA.
- [14] Jeong, J., Choi, C. (May 29-31.2008). Comparison of Wind Loads on Buildings using Computational Fluid Dynamics, Design Codes, and Wind Tunnel Tests. *Theth International Conference on Advances in Wind and Structures, Jeju, Korea*.
- [15] Tehrani, F. B., Ghafuri, A., Jadidi, M. (2013). Grid resolution assessment in large eddy simulation of dispersion around an isolated cubic building. *Journal of Wind Engineering and Industrial Aerodynamics*, 121, 1-15.
- [16] Özdoğan, M., Sungur, B., Namli, L., Topaloğlu, B., Durmuş, A. (Kasım-Aralık 2015). Rüzgâr Hızlarının Bina Etrafındaki Akışa ve Isı Kaybına Etkisinin Farklı Türbülans Modelleriyle Sayısal İncelenmesi. *TTMD Dergisi*, 56-62.
- [17] Ansys Fluent UDF Manual. (2013). Release 15.0, ANSYS Inc, Canonsburg, PA.
- [18] Çelik Yapıların Tasarım, Hesap ve Yapım Dair Esaslar. (04.02.2016). Çevre ve Şehircilik Bakanlığı, Ankara.